**Rare Metal Materials and Engineering**
Volume 49, Issue 2, February 2020
Available online at www.rmme.ac.cn

Science Press

**Cite this article as:** Rare Metal Materials and Engineering, 2020, 49(2): 0391-0397.

ARTICLE

# Superplastic Deformation Mechanism and Simultaneous Microstructure Evolution of Fine-grained Ti-6Al-4V Wide Sheet

**Zhang Xuehua[1,2], Zhao Yongqing[1,3], Zeng Weidong[1]**

*[1] State Key Laboratory of Solidification Processing, Northwestern Polytechnical University, Xi'an 710072, China; [2] Western Metal Materials Co., Ltd, Xi'an 710021, China; [3] Northwest Institute for Nonferrous Metal Research, Xi'an 710016, China*

**Abstract:** The superplasticity of fine-grained Ti-6Al-4V wide sheet was investigated by constant strain rate tensile method. The superplastic tensile tests were carried out at temperatures ranging from 1103 K to 1223 K and strain rates ranging from $3.2\times10^{-4}$ $s^{-1}$ to $1\times10^{-2}$ $s^{-1}$. The results show that tensile elongation to failure values between 100% and 604% are obtained. Microstructure evolution and deformation mechanism were analyzed. Results show that the main deformation mechanism is grain boundary sliding, accommodated by matrix dislocation movement and the intragranular slip of $\beta$ phase. It is also found that the Ti-6Al-4V wide sheet shows anisotropy when deformed at lower temperatures, which is obviously reduced when deformed at higher temperatures.

**Key words:** Ti-6Al-4V wide sheet; superplasticity; deformation mechanism; anisotropy

Ti-6Al-4V alloy is extensively applied in the aerospace, marine and chemical industries owing to its high specific strength, high plasticity, superior corrosion and high temperature resistances[1-6]. However, its high deformation resistance and severe processing rebound hinder the manufacture of products such as wide and thin sheets[7]. Superplastic forming process can greatly reduce the deformation resistance, and may be used to produce precision parts with complex shapes[8]. Thus, Ti-6Al-4V wide sheets with superplasticity are of great significance for the preparation of large aeronautical components.

In the past few years, the superplastic properties of many titanium alloys have been investigated[7-18]. It is generally accepted that the process variables such as grain-size configuration, strain rate and temperature have great influences on the final microstructures and mechanical properties of the products formed. The major superplastic deformation mechanism has been attributed to grain boundary sliding (GBS) and its accommodation process[17]. Nevertheless, most researches are focused on the simple bars or small plates, and there is only scarce work on large plates. Some obvious differences are certain to appear between the test results of small plates and wide sheets, where anisotropy is a direct evidence.

In the present work, tensile specimens were taken directly from Ti-6Al-4V wide sheets in supply state. The superplastic deformation behavior and the difference of transverse and longitudinal properties were investigated. Moreover, the concurrent microstructure evolution mechanism was explored to reveal the correlation of deformability and structure.

## 1 Experiment

The Ti-6Al-4V sheet used with an original size of 1.2 mm×1000 mm×2000 mm was provided by Western Metal Materials Co., Ltd. Its chemical composition is Ti-6.16Al-4.17V-0.062Fe-0.009C-0.003N-0.002H-0.15O (wt%) and the $\alpha/\beta$ transition temperature is about 1253 K. The initial microstructure of this alloy sheet is shown in Fig.1a, where the mean grain size of $\alpha$ is approximately 3 μm. Transverse and longitudinal specimens were cut from the original sheet. The sampling direction and dimension of the specimen are presented in Fig.1b and 1c.

Received date: February 06, 2019
Foundation item: National Natural Science Foundation of China (51471136)
Corresponding author: Zhao Yongqing, Professor, Northwest Institute for Nonferrous Metal Research, Xi'an 710016, P. R. China, Tel: 0086-29-86231105, E-mail: trc@c-nin.com

Copyright © 2020, Northwest Institute for Nonferrous Metal Research. Published by Science Press. All rights reserved.

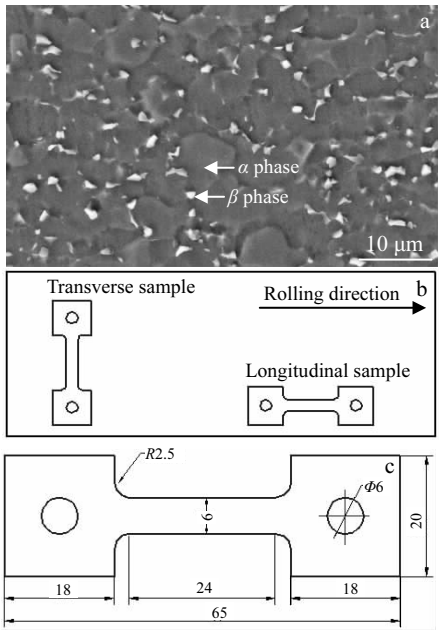


Fig.1 Microstructure of initial Ti-6Al-4V alloy sheet (a) and schematic illustration of tensile test specimen (mm) (b, c)

Superplasticity tensile tests were carried out on a CMT4104 electronic tensile machine in air. Tensile testing temperatures and strain rates ranged from 1103 K to 1223 K and $3.2\times10^{-4}$ $s^{-1}$ to $1\times10^{-2}$ $s^{-1}$, respectively. Glass-protective lubricants were used to prevent the oxidation.

The specimens were heated to the target temperatures, held for 5 min, and then elongated up to fracture and quenched in water immediately. Their final microstructures were observed by an optical microscope (OM, ZEISS 40MAT), scanning electron microscope (SEM, ZEISS SUPRA 55) and transmission electron microscope (TEM, JEM-200CX)

## 2 Results and Discussion

### 2.1 Superplasticity during tensile deformation

The true stress-strain curves of Ti-6Al-4V alloy obtained by tensile tests at temperatures ranging from 1103 K to 1223 K and strain rates from $3.2\times10^{-4}$ $s^{-1}$ to $1\times10^{-2}$ $s^{-1}$ are shown in Fig.2. The long strain hardening stages are observed at all tensile conditions, and the peak stress decreases monotonically with the increase of deformation temperature and the decrease of strain rate. When deformed at 1163 K, the maximum stress is 59 MPa at $1\times10^{-2}$ $s^{-1}$, and meanwhile the minimum stress is only 20 MPa at $3.2\times10^{-4}$ $s^{-1}$ (Fig.2b).

It is known that high temperature can increase the atom activity and reduce the grain boundary viscous force, and thus make the grain boundary sliding easier. Meanwhile, high temperature and low strain rate can promote $\alpha\rightarrow\beta$ phase transformation, resulting in the increase of the proportion of the $\beta$ phase which is easily deformed. In addition, high temperature can accelerate the dislocation movement and low strain rate may provide sufficient time for dislocation migration and annihilation, which can effectively coordinate grain boundary sliding and decrease dislocation density. Therefore, both increasing temperature and decreasing strain rate can reduce the strain stress, as shown in Fig.2.

Arrhenius equation can be used to describe the relationship

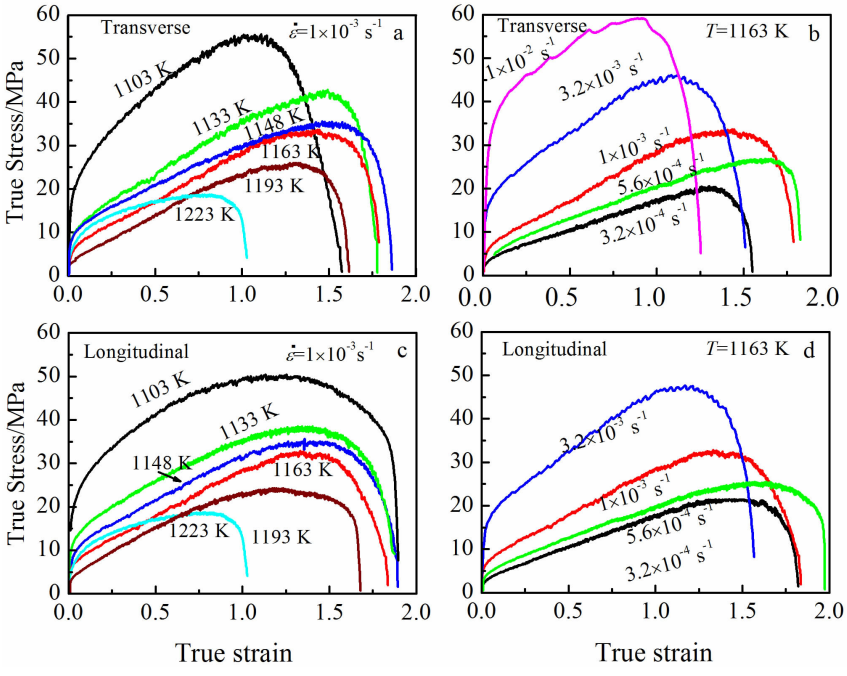


Fig.2 True stress-strain curves of transverse (a, b) and longitudinal (c, d) samples

between the flow stress σ and the strain rate $\dot{\varepsilon}$ [19,20]:

$$\dot{\varepsilon} = A\sigma^{1/m}\exp(-\frac{Q}{RT}) \quad (1)$$

Moreover, $m$ and $Q$ can be obtained by follows:

$$m = \left.\frac{\mathrm{d}\ln\sigma}{\mathrm{d}\ln\dot{\varepsilon}}\right|_T \quad (2)$$

$$Q = R\left[\frac{\partial\ln\sigma}{\partial(1/T)}\right]_{\dot{\varepsilon}}\left[\frac{\partial\ln\dot{\varepsilon}}{\partial\ln\sigma}\right]_T \quad (3)$$

where $\dot{\varepsilon}$ is strain rate, $m$ is strain rate sensitivity index, $Q$ is activation energy, $A$ is a material constant, $\sigma$ is true stress, $R$ is gas constant and $T$ is absolute temperature[19,20].

The true stress versus strain rate and temperature is shown in Fig.3. The $Q$ and $m$ values of Ti-6Al-4V alloy were calculated through Eq.(2) and Eq.(3). The strain rate sensitivity indexes $m$ of both longitudinal and transverse samples are 0.35. The activation energy of longitudinal sample $Q_L$ is 244 kJ/mol and that of transverse one $Q_T$ is 266 kJ/mol. Both of them are higher than the activation energy of the self-diffusion of $\alpha$-Ti (204 kJ/mol) and $\beta$-Ti (161 kJ/mol)[21]. $Q_L$ is lower than $Q_T$, indicating that the deformation is easier when the direction of tensile stress is consistent with the original rolling direction.

The elongation to fracture is an important characteristic parameter of the plastic deformation capability. The elongation to fracture of Ti-6Al-4V alloy under different deformation conditions is presented in Fig.4. It can be clearly seen that at

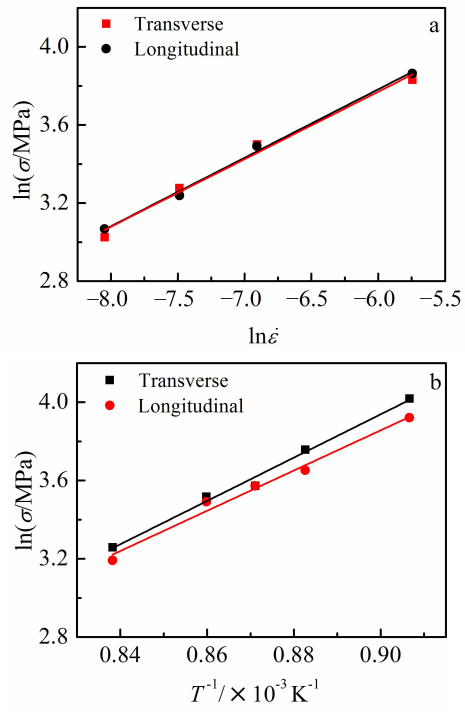


Fig.3 True stress $\sigma$ versus strain rate $\dot{\varepsilon}$ and temperature $T$: (a) ln$\sigma$-ln$\dot{\varepsilon}$ and (b) ln$\sigma$-$T^{-1}$

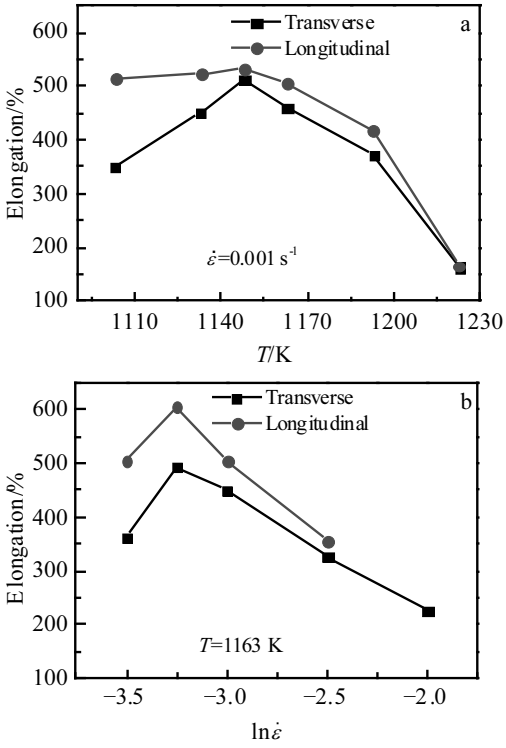


Fig.4 Effect of temperature (a) and strain rate (b) on the elongation of Ti-6Al-4V alloy sheet

the strain rate of $1\times10^{-3}$ $s^{-1}$, for both transverse and longitudinal specimens, the elongation increases first and then decreases with the rise of temperature. And at low temperatures, the elongation of longitudinal specimens is higher than that of transverse specimens. There is no significant difference at high temperatures, as shown in Fig.4a. When deformed at 1163 K, for all the samples, the elongation firstly increases and then decreases with the increment of initial strain rate. As illustrated in Fig.4b, the maximum elongation of 604% is obtained at an initial strain rate of $5.6\times10^{-4}$ $s^{-1}$.

### 2.2 Microstructure evolution accompanying superplastic deformation

#### 2.2.1 Effect of deformation degree

It is shown in Fig.5 that after deformation at 1148 K with the strain rate of $1\times10^{-3}$ $s^{-1}$, both $\alpha$ and $\beta$ grains are much coarser than the initial grains. The average grain size increases from 3.0 μm to 5.4 μm in the middle section, while it ranges from 3.0 μm to 4.2 μm in the grip section. The volume fraction of $\beta$ phase at the gauge section is larger than at the grip section. In the tensile process, the grip section of the specimen is not affected by tensile stress, and thus the grain growth here is caused by thermal effects. In contrast, the middle region of the sample is affected by both tensile stress and heat treatment. It is obvious that the grain growth and phase transformation are influenced significantly by the stress during superplastic deformation.

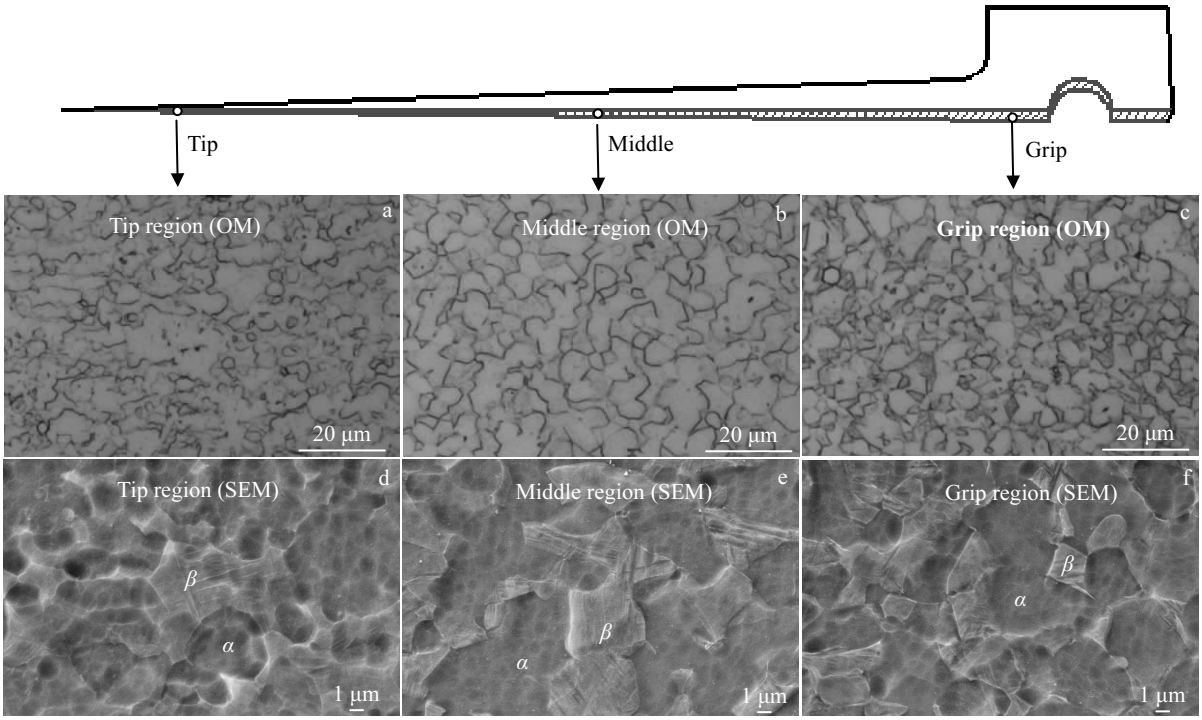


Fig.5 OM and SEM images of the longitudinal sample after superplastic deformation at 1148 K with the strain rate of $1\times10^{-3}$ $s^{-1}$: (a, d) tip region, (b, e) middle region, and (c, f) grip region

Furthermore, fine-equiaxed grains are found in the microstructure of the tip section, which means that dynamic recrystallization is induced by large deformation, as shown in Fig.5a and Fig.5d.

2.2.2 Effect of deformation temperature

Fig.6 presents the TEM images of deformed longitudinal samples with the strain rate $1\times10^{-3}$ $s^{-1}$ at different temperatures. After deformation at 1103 K, dislocations are found near the grain boundaries and inside the $\alpha$ grains. The $\alpha/\beta$ interfaces turn to be arc-shaped and distorted after deformation, as shown in Fig.6a~6c. Recrystallized grains are also found in Fig.6a, which indicates that dynamic recrystallization (DRX) occurs during superplastic deformation.

As compared with the microstructures deformed at 1103 K, the volume fraction of $\beta$ phase in the microstructure after deformation at 1148 K is obviously increased, as shown in Fig.6d and 6e. It can be seen that the $\alpha/\alpha$ grain boundary is straight with few dislocations, whereas there are many dislocations at the $\alpha/\beta$ grain boundary. The $\alpha/\beta$ grain boundaries become curved obviously, which are typical characteristics of superplastic deformation [22]. Moreover, it is seen that $\beta$ phase inserts $\alpha$ grain boundaries and some $\alpha$ grain boundaries are replaced by $\alpha/\beta$ interfaces, as shown by the arrow in Fig.6e. The suitable volume fraction of $\beta$ phase at this temperature is beneficial to superplastic deformation, resulting in good elongation.

When the temperature is elevated to 1193 K, $\alpha\rightarrow\beta$ phase transition occurs obviously, which evidently leads to the decrease in the volume fraction of primary $\alpha$ phase. Meanwhile, as shown in Fig.6f, the grains grow up together into larger grains, which reduce the interface of slip deformation. Thus the elongation decreases obviously.

In order to reveal the reasons for the difference in transverse and longitudinal properties after superplastic deformation at low temperatures, the transverse specimens deformed at 1103 K and $1\times10^{-3}$ $s^{-1}$ were also analyzed by TEM, as shown in Fig.7. Compared with longitudinal sample (Fig.6a~6c), the transverse sample has a higher dislocation density. The dislocation walls and sub-boundary appear in elongated grains (Fig.7a), while dislocation network exists in large grains (Fig.7b) and lots of dislocations at phase boundaries are tangled (Fig.7c), which indicates that the grain boundary movement is more difficult and may be responsible for the serious strain hardening and lower elongation.

2.2.3 Effect of strain rate

Fig.8 provides the microstructure of longitudinal samples deformed at 1163 K with different strain rates. Along with the decrease of strain rate, $\alpha$ grain size and the volume fraction of $\beta$ phase increase obviously after deformation, as indicated in Fig.8a~8c. After deformation at $3.2\times10^{-4}$ $s^{-1}$, the grains are coarsened badly due to a long time holding at high temperatures. The coarsened microstructure is not beneficial to superplastic deformation, and hence the elongation of samples deformed at $3.2\times10^{-4}$ $s^{-1}$ is lower than at $5.6\times10^{-4}$ $s^{-1}$(Fig.4b).

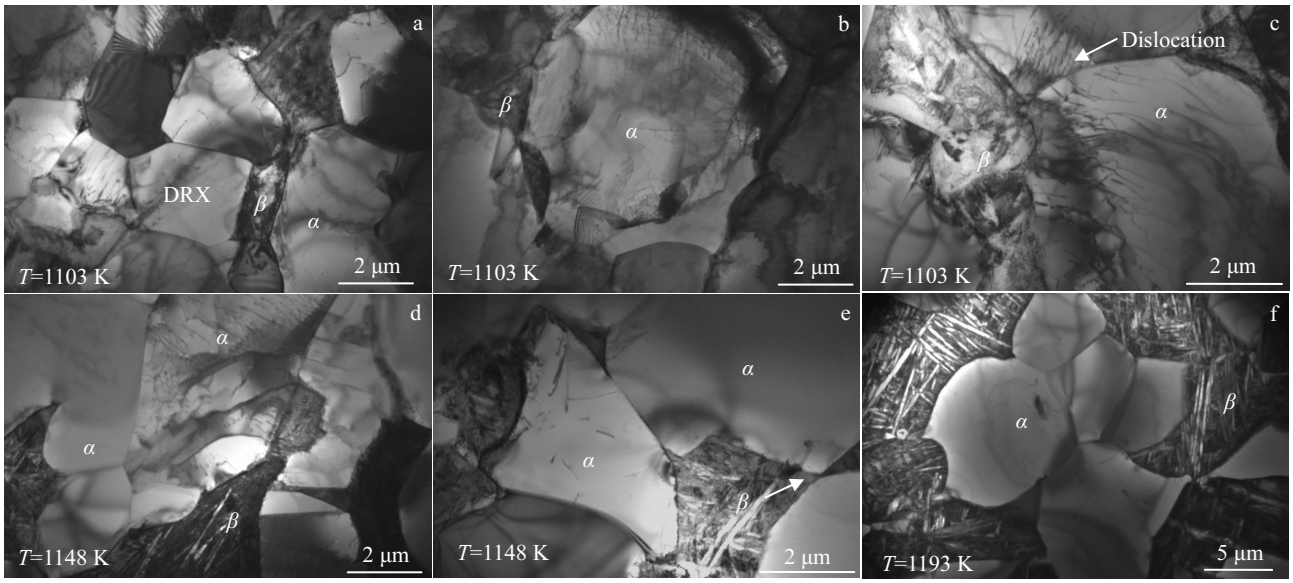


Fig.6 TEM images of deformed longitudinal samples with the strain rate $1\times10^{-3}$ $s^{-1}$ at different temperatures: (a~c) 1103 K, (d, e) 1148 K, and (f) 1193 K

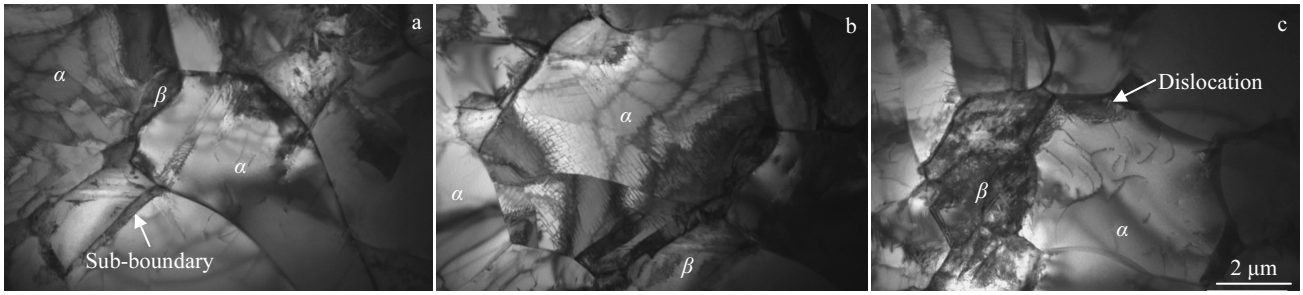


Fig.7 TEM images of deformed transverse samples with the strain rate $1\times10^{-3}$ $s^{-1}$ at 1103 K: (a) dislocation walls and sub-boundary, (b) dislocation network, and (c) tangled dislocations

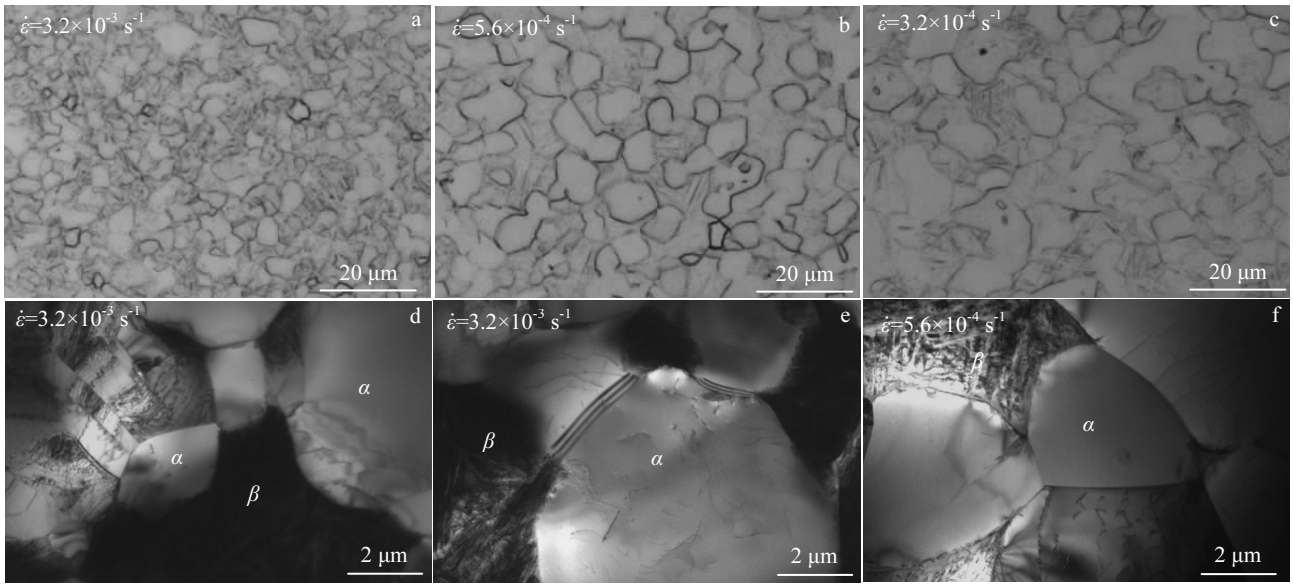


Fig.8 OM and TEM images of longitudinal samples deformed at 1163 K with different strain rates: (a, d, e) $3.2\times10^{-3}$ $s^{-1}$, (b, f) $5.6\times10^{-4}$ $s^{-1}$ and (c) $3.2\times10^{-4}$ $s^{-1}$

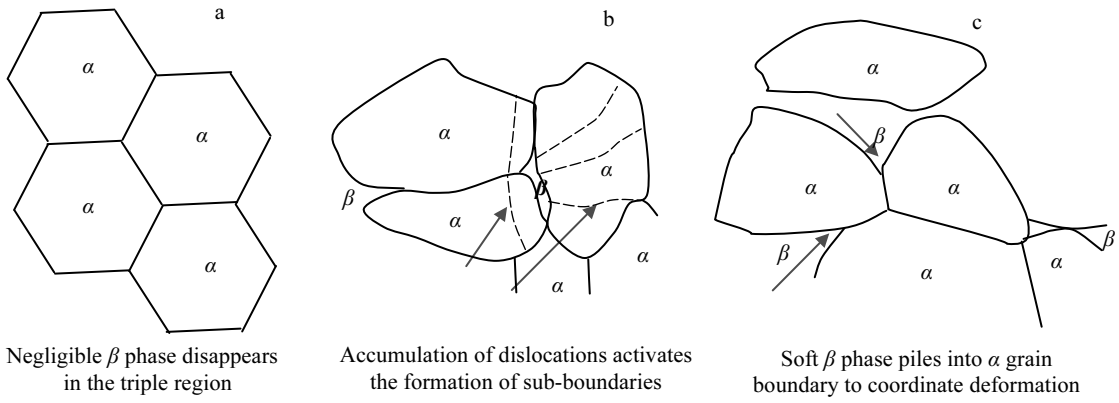


Fig.9 Schematic of superplastic deformation mechanism for Ti-6Al-4V alloy: (a) initial microstructure, (b) deformed at 1103 K with $1\times10^{-3}$ $s^{-1}$ and (c) deformed at 1163 K with $5.6\times10^{-4}$ $s^{-1}$

A detail observation of the deformed grains was carried out by the TEM, as presented in Fig.8d~8f. After deformation at $3.2\times10^{-3}$ $s^{-1}$, planar arrays of dislocations and parallel dislocation lines appear in large $\alpha$ grains (Fig.8d and 8e). The pilling up of dislocations hinders the grain boundary sliding, and causes the stress concentration, which is not beneficial to uniform deformation. After deformation at $5.6\times10^{-4}$ $s^{-1}$, $\alpha/\beta$ phase boundary exhibits curved and distorted morphology, while $\alpha/\alpha$ grain boundary exhibits straight feature, and $\beta$ phase piles into $\alpha$ phase and $\alpha/\alpha$ grain boundaries, trying to surround $\alpha$ grains to harmonize the deformation (Fig.8f).

### 2.3 Deformation mechanism and anisotropy

Based on the above microstructure analysis of Ti-6Al-4V alloy, a simple sketch of superplastic deformation mechanism is proposed, as shown in Fig.9. The deformation mechanism is mainly grain boundary sliding (GBS), accommodated by different coordination modes under various deformation conditions.

When deformed at lower temperature or higher strain rate, $\alpha$ grains play the dominant role in deformation. The matrix dislocation motion and dynamic recrystallization in $\alpha$ phase are the main accommodating mechanisms. The intragranular dislocation movement of $\alpha$ phase can accommodate the grain boundary sliding, while the accumulation of dislocations activates the formation of sub-grains in big grains. If the deformation continues, the dynamic recrystallization will occur, as shown in Fig.9b.

When deformed at higher temperatures and lower strain rates, the $\beta$ phase increases. The $\beta$ phase can deform easily and undergo larger plastic deformation than $\alpha$ phase [23], In the process of superplastic deformation, the $\beta$ phase tends to surround $\alpha$ grains to coordinate the deformation, as shown in Fig.9c. Thus, the accommodation mechanism is the intragranular slip of $\beta$ phase.

The Ti-6Al-4V wide sheet was prepared by multi-step hot-rolling. Although several reversals were carried out in the rolling process, anisotropy was also found in the experiment. The elongation of longitudinal sample is higher than that of the transverse one under the same deforming conditions, especially at lower temperatures. In the in-situ tensile test, it was also found that the tensile property of longitudinal specimen is better than that of the transverse one[24].

When deformed at 1103 K and$1\times10^{-3}$ $s^{-1}$, the true stress of transverse sample increases more quickly to the peak stress than that of the longitudinal one, and then sharply drops down, which indicates that serious strain hardening has occurred. The peak stress of transverse sample (56 MPa) is higher than that of the longitudinal sample (50 MPa), and the elongation to fracture of transverse sample (350%) is much lower than that of the longitudinal sample (513%), as shown in Fig.2 and Fig.4. Moreover, for the longitudinal samples, as shown in Fig.6c, dislocations are extended into $\alpha$ grains from the $\alpha/\beta$ phase boundaries, which can relax stress concentration. However, for the transverse samples, as presented in Fig.7c, lots of dislocations at phase boundaries are tangled, which indicates that the grain boundary movement is more difficult and may be responsible for serious strain hardening and lower elongation.

The initial reasons why the dislocations in the transverse sample are more difficult to move may be due to the texture which was formed in the hot-rolling process. The influence of texture on the anisotropy of this alloy sheet is worth further investigations.

When the temperature is enhanced to above 1148 K, there is almost no difference in elongation between longitudinal and transverse specimens. This may be due to the fact that the high temperature annealing of warm rolled Ti-6Al-4V alloy generally modifies the relative strength of texture fibers [9]. In order to avoid the effect of anisotropy on the shape of products, it is suggested that the Ti-6Al-4V wide sheet should be superplastically formed at above 1148 K.

## 3 Conclusions

1) The fine grained Ti-6Al-4V sheet exhibits good superplasticity in the temperature ranging from 1103 K to 1223 K with strain rates varying from $3.2\times10^{-4}$ $s^{-1}$ to $1\times10^{-2}$ $s^{-1}$. The elongation increases at first and then decreases with the rise of temperature and the reduction of strain rate. The maximum elongation of 604% is obtained at 1163 K and $5.6\times10^{-4}$ $s^{-1}$.

2) The deformation mechanism is mainly grain boundary sliding (GBS), accommodated by dislocation movement and dynamic recrystallization at lower temperature or higher strain rate. When the deformation temperature is above 1148 K and the strain rate is below $1\times10^{-3}$ $s^{-1}$, the deformation mechanism is further facilitated by the intragranular slip of $\beta$ phase.

3) For Ti-6Al-4V alloy wide sheet, the longitudinal samples show higher elongation than transverse ones, especially when deformed at lower temperatures. The anisotropy can be reduced when the deform temperature exceeds 1148 K.

## References


1 Zhou K, Wei B. *Applied Physics A*[J], 2016, 122: 248
2 Roy S, Suwas S. *Materials and Design*[J], 2014, 58: 52
3 Shahmir H, Langdon T G. *Acta Materialia*[J], 2017, 141: 419
4 Bruschi S, Poggio S, Quadrini F *et al*. *Materials Letters*[J], 2004, 58(27-28): 3622
5 Feng X, Qiu J K, Ma Y J *et al*. *Journal of Materials Science & Technology*[J], 2016, 32 (4): 362
6 Salem A A, Glavicic M G, Semiatin S L. *Materials Science and Engineering A*[J], 2008, 496: 169
7 Zhang T Y, Liu Y, Sanders D G *et al*. *Materials Science and Engineering A*[J], 2014, 608: 265
8 Alabort E, Putman D, Reed R C. *Acta Materialia*[J], 2015, 95: 428
9 Roy S, Suwas S. *Materials Science and Engineering A*[J], 2013, 574: 205
10 Matsumoto H, Yoshida K, Lee S H *et al*. *Materials Letters*[J], 2013, 98: 209
11 Zherebtsov S V, Kudryavtsev E A, Salishchev G A *et al*. *Acta Materialia*[J], 2016, 121: 152
12 Motyka M, Sieniawski J, Ziaja W. *Materials Science and Engineering A*[J], 2014, 599: 57
13 Lee C S, Lee S B, Kim J S *et al*. *International Journal of Mechanical Sciences*[J], 2000, 42(8): 1555
14 Alabort E, Kontis P, Barba D *et al*. *Acta Materialia*[J], 2016, 105: 449
15 Xiao M J, Tian Y X, Mao G W *et al*. *Journal of Materials Science & Technology*[J], 2011, 27(12): 1099
16 Zhang X M, Cao L L, Zhao Y Q *et al*. *Materials Science and Engineering A*[J], 2013, 560: 700
17 Kim J S, Kim J H, Lee Y T *et al*. *Materials Science and Engineering A*[J], 1999, 263: 272
18 Shahmir H, Naghdi F, Pereira P H R *et al*. *Materials Science and Engineering A*[J], 2018, 718: 198
19 Sun Q J, Wang G C. *Materials Science and Engineering A*[J], 2014, 606: 401
20 Zhang X M, Zhao Y Q, Zeng W D. *Materials Science and Engineering A*[J], 2010, 527(15): 3489
21 Meier M L, Lesuer D R, Mukherjee A K. *Materials Science and Engineering A*[J], 1991, 136: 71
22 Sergueeva A V, Stolyarov V V, Valiev R Z *et al*. *Materials Science and Engineering A*[J], 2002, 323: 318
23 Liu Z G, Li P J, Xiong L T *et al*. *Materials Science and Engineering A*[J], 2017, 680: 259
24 Zhang X H, Zhang S Y, Zhao Q Y *et al*. *Journal of Alloys and Compounds*[J], 2018, 740: 660


# 细晶 Ti-6Al-4V 宽幅板材的超塑性变形机理及组织演变


张雪华[1,2]，赵永庆[1,3]，曾卫东[1]

(1. 西北工业大学 凝固技术国家重点实验室，陕西 西安 710072)

(2. 西部金属材料股份有限公司，陕西 西安 710021)

(3. 西北有色金属研究院，陕西 西安 710016)



**摘　要**：通过恒应变速率拉伸试验，在 1103~1223 K 温度范围、$3.2\times10^{-4}$~$1\times10^{-2}$ $s^{-1}$ 应变速率范围内，研究了 Ti-6Al-4V 宽幅板材的超塑性，在实验中获得了 100%~604%的延伸率。分析了组织演变和变形机理，结果表明，其主要变形机理为晶界滑移，以晶内位错运动和 $\beta$ 相的晶内滑移为协调机制。实验中还发现在低温下变形时，Ti-6Al-4V 宽幅板材存在各向异性，当在高温下变形时，各向异性不太明显。



**关键词**：Ti-6Al-4V 宽幅板材；超塑性；变形机理；各向异性



作者简介：张雪华，女，1982 年生，博士生，西部金属材料股份有限公司，陕西 西安 710072，电话：029-86968705，E-mail: zxhxyt@126.com